

---

# Global Optimization of $\text{Si}_x\text{H}_y$ at the Ab Initio Level via an Iteratively Parametrized Semiempirical Method

---

YINGBIN GE, JOHN D. HEAD

*Department of Chemistry, University of Hawaii, 2545 The Mall, Honolulu, Hawaii 96822*

*Received 28 March 2003; accepted 8 April 2003*

*DOI 10.1002/qua.10630*

---

**ABSTRACT:** Previously we searched for the ab initio global minima of several  $\text{Si}_x\text{H}_y$  clusters by a genetic algorithm in which we used the AM1 semiempirical method to facilitate a rapid energy calculation for the many different cluster geometries explored. However, we found that the AM1 energy ranking significantly differs from the ab initio energy ranking. To better guarantee locating the ab initio global minimum while retaining the efficiency of the AM1 method, we present an improved iterative global optimization strategy. The method involves two separate genetic algorithms that are invoked consecutively. One is the cluster genetic algorithm (CGA), mentioned above, to find the semiempirical  $\text{Si}_x\text{H}_y$  cluster global minimum. A second and separate parametrization genetic algorithm (PGA) is used to reparametrize the AM1 method using some of the ab initio data generated from the CGA to form a training set of different reference clusters but with fixed  $\text{Si}_x\text{H}_y$  stoichiometry. The cluster global optimization search (CGA) and the semiempirical parametrization (PGA) steps are performed iteratively until the semiempirical GA reparametrized AM1 (GAM1) calculations give low-energy optimized structures that are consistent with the globally optimized ab initio structure. We illustrate the new global optimization strategy by attempting to find the ab initio global minima for the  $\text{Si}_6\text{H}_2$  and  $\text{Si}_6\text{H}_6$  clusters. © 2003 Wiley Periodicals, Inc. *Int J Quantum Chem* 95: 617–626, 2003

**Key words:** ab initio method; genetic algorithm; global optimization; hydride; parametrization; semiempirical method

---

## Introduction

Nanometer-sized Si particles have attracted much interest due to their potential optoelectronic properties, which could be useful in various

technological applications. We anticipate that such a device would contain silicon clusters whose surfaces are passivated by some chemically inert ligands. In this article we theoretically examine H atoms as passivation ligands and investigate the low-energy structures and stabilities of  $\text{Si}_x\text{H}_y$  clusters. The H atom serves as a prototype ligand because  $\text{Si}_x\text{H}_y$  clusters are generally unstable in the

*Correspondence to:* J. D. Head; e-mail: johnh@hawaii.edu

air. There have been a number of other studies on  $\text{Si}_x\text{H}_y$  clusters. Chambreau et al. [1] performed flash pyrolysis of silane and disilane to produce  $\text{Si}_x\text{H}_y$  clusters in studies of chemical vapor deposition (CVD). The authors also used second-order Møller–Plesset (MP2) calculations to predict the geometries and relative stabilities of three  $\text{Si}_6\text{H}$  and five  $\text{Si}_6\text{H}_2$  clusters by starting from geometries built by adding one or two H atoms onto the stable  $\text{Si}_6$  cluster with  $D_{4h}$  symmetry. Unfortunately, the investigators were not able to ascertain whether their fabricated  $\text{Si}_6\text{H}$  and  $\text{Si}_6\text{H}_2$  clusters actually are the most stable structures. Meleshko et al. [2] also attempted to identify global minima for various silicon hydride clusters using simulated annealing and the MINDO/3 method to evaluate the cluster energy. Due to the inaccuracy of the MINDO/3 semiempirical method when compared against ab initio methods, it is questionable if the authors obtained the true  $\text{Si}_x\text{H}_y$  global minima. Miyazaki et al. [3] used density functional theory–based methods to study the stable structures of  $\text{Si}_6\text{H}_{2n}$  ( $n = 1-7$ ). Their search for the local minima was started by using a combination of simulated annealing with pseudopotentials for Si and H atoms, along with optimizing structures initially built using chemical intuition, and by considering structures previously proposed by others.

Recently we developed a global optimization strategy based on a genetic algorithm (GA) for theoretically investigating the structures of partially and completely H-passivated Si clusters [4]. Because our global minimum search entails many cluster energy evaluations, we used the computationally fast AM1 semiempirical method [5] to identify the most stable  $\text{Si}_x\text{H}_y$  cluster, along with a number of low-energy isomers. The AM1 energy calculation has the important feature of a solid quantum mechanical basis so that no additional empirical information is needed to identify which atom pairs in the binary  $\text{Si}_x\text{H}_y$  cluster combine to form bonds. Nonetheless, we expect ab initio calculations at either the MP2 [6] or the density functional theory with Becke's three-parameter exchange functional and the gradient-corrected functional of Lee, Yang, and Paar (B3LYP) functional levels [7] to better predict structures closer to experimental reality. In our previous work we hoped by evaluating the ab initio energy for the various low-energy AM1 structures found by the GA that we could identify the most stable  $\text{Si}_x\text{H}_y$  cluster at the ab initio level. The original AM1 parameters for Si were determined from a limited

number of small molecules containing one or a few Si atoms [8], where the Si atoms were mostly four-coordinate bonded. Thus, it is not surprising that the AM1 parameters may fail to correctly rank the relative energies of Si clusters that have surface atoms not fully passivated or that have great ring strain. However, we also found that the low-energy AM1 structures of the fully H-passivated Si clusters obtained by the global optimization were too close in relative energies when compared against the ab initio energies, making it difficult to guarantee that the set of low-energy AM1 structures always includes the ab initio global minimum. The AM1 method performs even worse when it is applied to evaluation of the relative stabilities of barely H-passivated Si clusters. We find that the  $\text{Si}_6\text{H}_2$  AM1 global minimum adopts a linear structure even though the ab initio calculations predict the linear structure to be highly unstable relative to the more compact structures, such as  $D_{4h}$   $\text{Si}_6$  cluster with two H atoms each on one apex. Most of the other low-AM1-energy clusters adopt partially linear structures containing many Si atoms with only two-fold coordination, which are also determined as unstable structures with high ab initio energies. Thus, our strategy is not able to locate the ab initio low-energy clusters if we select only from the top 10 or 20 AM1 low-energy clusters to perform ab initio calculations. In this article we present an improved iterative global optimization strategy based on using semiempirical calculations that should better converge to the correct ab initio energetic ranking. The method involves using two separate GAs that are invoked consecutively. The first GA, the CGA, corresponds to the previous GA we developed to find the  $\text{Si}_x\text{H}_y$  cluster global minimum [4]. A second and separate PGA is used to reparametrize the AM1 method against ab initio data, which is generated as we attempt to find the ab initio global minimum. The GA-reparametrized AM1 (GAM1) semiempirical method is intended to better reproduce the ab initio energetics of the clusters with a specific  $\text{Si}_x\text{H}_y$  stoichiometry contained in the training set.

Genetic algorithms have been used previously to find parameters for semiempirical methods. Rossi and Truhlar [9] used a GA to obtain specific-reaction parameters (SRP) for use in dynamics calculations on the  $\text{Cl} + \text{CH}_4 \rightarrow \text{HCl} + \text{CH}_3$  reaction. The NDDO-SRP parameters were obtained by fitting to reference ab initio data calculated at relevant points along the specific reaction pathway. Cundari et al. optimized the PM3 [10] parameters of Tc using a GA to match the PM3 optimized geometries of the

Tc compounds with their crystal structures by comparing their atom distances [11]. Their GA-revised PM3 parameters significantly improved the performance compared with the original PM3 parameters, which were obtained by the interpolation of the parameters for Mo and Ru. Our approach resembles the strategy proposed by Hartke of iteratively modifying an empirical potential for Si clusters against the true cluster energy calculated by some ab initio method [12]. As a preliminary test for this strategy, Hartke used the Stillinger–Weber potential [13] with modifications by Gong [14] for the empirical potential and another empirical potential by Bolding and Anderson [15] to simulate the ab initio energy [12]. More recently, Hartke [16] applied this approach to find the global minima of small Si clusters using density functional theory as the true cluster energy. In the current work, we use the MP2 ab initio method to define the true cluster energy. Rather than having a fixed training set for the specific  $\text{Si}_x\text{H}_y$  cluster type, we adopt the idea by Hartke of expanding the training set used in the GAM1 parametrization iteratively. We first use the CGA to generate around 50 to 60 structures to be included in the training set used by the PGA. Once a set of GAM1 parameters is obtained by the PGA, we repeat the CGA to find the set of lowest-energy clusters derived from the new semiempirical parameters. Any new cluster structures generated are iteratively included in the training set and the parametrization is repeated with the PGA to obtain the next GAM1 parameters. The cluster global optimization at the ab initio level is repeated for at least five GAM1 parameter optimization cycles and is continued until a consistent set of low-energy clusters is obtained.

In the next section we describe in more detail how the ab initio global optimization strategy is implemented, along with a description of the two coupled GAs. We then illustrate examples of the global optimization strategy for the  $\text{Si}_6\text{H}_2$  cluster with low H passivation and  $\text{Si}_6\text{H}_6$  cluster with medium H passivation. We include a comparison with the previously found low-energy  $\text{Si}_6\text{H}_2$  and  $\text{Si}_6\text{H}_6$  structures. Concluding remarks are given in the final section.

---

## Computational Method

The determination of the global optimization of  $\text{Si}_x\text{H}_y$  at the ab initio level consists of five main steps, outlined as follows.

### 1. INITIAL TRAINING SET DESIGN

We perform an initial crude cluster global optimization of the  $\text{Si}_x\text{H}_y$  cluster and terminate it prematurely once 50 unique AM1 locally optimized geometries are generated. We visually examine any two AM1 optimized geometries that have energy differences of less than 0.1 kcal/mol for distinct structures. This step is intended to generate a number of different  $\text{Si}_x\text{H}_y$  clusters with different structural features spread over an approximately 100 kcal/mol energy range. In contrast, cluster global optimization steps are intended to generate structures with low energies. We do not adopt the idea by Hartke of simply generating random training compounds, because we find Si hydrides have a more complicated potential energy surface than do bare Si clusters. Many of our randomly generated structures have high MP2 energies. We find both low- and high-energy structures are needed to ensure that the PGA finds new GAM1 parameters that reasonably match the MP2 energies for the more stable clusters. We then compute the single-point MP2 energies for the initial 50 training compounds. We also use the MP2 method to locally optimize the five geometries with the lowest single-point MP2 energies. To speed up these MP2 optimizations we use reduced convergence conditions with the maximum gradient  $< 10^{-3}$  a.u. and root mean square (RMS) gradient  $< 0.33 \times 10^{-3}$  a.u. We find that the reduced convergence criterion usually gives MP2 energies within 0.1 kcal/mol of those obtained by the default General Atomic and Molecular Electronic Structure System (GAMESS) convergence condition (maximum gradient  $< 10^{-4}$  a.u. and RMS gradient  $< 0.33 \times 10^{-4}$  a.u.). The 50 AM1-optimized geometries and the five derived MP2 optimized geometries are all included in the training set for the first cycle of the GAM1 parametrization. We selectively exclude some unphysical clusters that have excessively high MP2 energies. Perhaps surprisingly, this criterion caused us not to include the linear  $\text{Si}_6\text{H}_2$  AM1 global minimum structure in the training set.

### 2. GAM1 PARAMETER OPTIMIZATION USING THE PARAMETRIZATION GA (PGA)

The semiempirical calculations are all performed using the original AM1 equations. We redetermine only the 16 parameters of the Si atom: the atomic core integrals  $U_{ss}$  and  $U_{pp}$ , the Slater-type orbital exponents  $\zeta_s$  and  $\zeta_p$ , the resonance  $\beta_s$  and  $\beta_p$ , the

core–core repulsion term  $\alpha$ , and the nine core repulsion function parameters ( $K_{1-3}$ ,  $L_{1-3}$ , and  $M_{1-3}$ ) [8].

Our experience suggests that a PGA with the population size 100 balances the efficiency and effectiveness of the optimization well. The initial 100 sets of different GAM1 parameters are randomly assigned values with a range of  $\pm 30\%$  from the original AM1 parameters. For each distinct parameter set, a GAM1 single-point energy is evaluated for every geometry in the training set. We define the fitness function  $f$  to be the RMS deviation between the GAM1 and MP2 single-point energies times a penalty coefficient  $P$ :

$$f = P \left[ \sum_{i=1}^{N_c} (E_i^{\text{GAM1}} - E_i^{\text{MP2}} + D)^2 / N_c \right]^{1/2} \quad (1)$$

where  $D$  is introduced as a displacement to minimize the RMS deviation between the GAM1 and MP2 relative energies:

$$D = \sum_{i=1}^{N_c} (E_i^{\text{MP2}} - E_i^{\text{GAM1}}) / N_c. \quad (2)$$

Because it is possible that some of the trial GAM1 parameters do not enable the self-consistent field (SCF) step to converge for all the training compounds, we evaluate the fitness function using the  $N_c$  training compounds reaching SCF convergence. We also introduce  $P$  as the penalty coefficient that takes into account when there are fewer SCF calculations reaching convergence:

$$P = e^{2.0(N_T - N_c) / N_T} \quad (3)$$

where  $N_T$  is the total number of the training compounds. The smaller is the fitness value, the better do our GAM1 energies match the ab initio energies.

After the initial 100 fitness values are obtained, the top 10% GAM1 parameter sets with the smallest fitness values are copied directly into the offspring generation. The top 30% (including the top 10% mentioned above) are put into the breeding pool with equal weight, whereas the least fit 70% are eliminated from the generation. Pairs of parents are randomly chosen from the breeding pool to perform the uniform crossover to generate the remaining 90% offsprings. Each gene of an offspring has a 50%–50% chance of inheriting the gene of one of the two parents at the same position. The population

size is kept constant during the evolution. A 6.25% (1 of 16 GAM1 parameters) rate of mutation is performed on every offspring. The mutation works by randomly picking up one parameter and changing its value randomly within  $\pm 20\%$ . The best fitness value in one generation drops rapidly during the first few generations and starts to converge after 10 to 20 generations. We perform the PGA for 50 generations to guarantee well converged final GAM1 parameters with a small fitness value. We then replace the previous AM1 or GAM1 parameters with the new GAM1 parameters and repeat the global optimization of the  $\text{Si}_x\text{H}_y$  cluster.

### 3. CLUSTER GLOBAL OPTIMIZATION USING THE CLUSTER GA (CGA)

This strategy is only briefly described here because it is essentially the same as our previous genetic algorithm used for globally optimizing the  $\text{Si}_x\text{H}_y$  clusters [4]. The global optimization starts from a few initial random structures of the Si clusters as our ancestor population. The fitness  $f_i$  of the  $i$ -th initial individual cluster is based on a Boltzmann distribution:

$$f_i = \exp\left(\frac{C - \text{BE}_i}{NRT}\right) \quad (4)$$

where  $\text{BE}_i$  is the optimized GAM1 cluster binding energy,  $-C$  is a constant whose value is set to be the lowest energy obtained from the initial  $N$  ancestors—and  $N$  is the total number of atoms in that molecule. The constant  $C$  is used to rescale the fitness  $f_i$  to avoid computational overflow. The variable  $RT$  is set to 0.2 eV/atom. Roulette selection is used to select  $N$  random parent couples for the next generation. The probability  $P_i$  of the  $i$ -th geometry being selected is determined by the normalized fitness of that cluster:

$$P_i = f_i / \sum_i f_i. \quad (5)$$

One mating method is to take the arithmetic mean of the cartesian coordinates from two parent geometries. The second method is to take a fragment of Si atoms from one parent and replace it with the fragment of the other parent with the same number of atoms and also cut a fragment of H atoms from one parent and replace it with a fragment of H atoms in the other parent with the same number of atoms.

The last method is to cut each parent into halves and then recombine one half from each parent to generate the offspring. The first and second mating processes produce drastic mutations, whereas the third method retains much of the local structures of both parents. The probabilities used for selecting the first, second, and third methods are 25%, 25%, and 50%, respectively. After the mating process,  $N$  offspring are generated and fully optimized again by the GAM1 method. We replace the least stable structure of its parent population with a new offspring if this offspring has relatively lower energy and it differs with all other parents to guarantee the variety of the population. The above procedure is repeated until the lowest-energy structure does not change for  $3N$  generations.

#### 4. AUGMENTATION OF THE TRAINING SET

After the CGA, we select 10 GAM1 local minima with the lowest GAM1 energies and evaluate their single-point MP2 energies. One GAM1 structure with the lowest MP2 single-point energy is optimized using the MP2 method. The above 10 new GAM1 structures and the derived MP2 optimized structure are all added to the training set and used in the next cycle of the GAM1 parametrization starting at step 2. At least five GAM1 parameterization cycles are performed using steps 2, 3, and 4 and the whole global optimization procedure is repeated until either the average single-point MP2 energies of the 10 lowest GAM1 energy clusters are converged to 10 kcal/mol or when at least half of the different GAM1 parameter sets predict the same global minimum.

#### 5. DETERMINATION OF RELATIVE STABILITIES OF THE LOWEST MP2 ENERGY CLUSTERS

After the final GAM1 parameters and the resulting low GAM1 energy clusters are found, we fully optimize the 10 clusters with lowest GAM1 energies at the MP2 level. From these 10 optimized structures along with consideration of the other previously optimized MP2 geometries, we select the ones with the lowest MP2 energies within a range of 20 kcal/mol. We then further compute the zero-point energy (ZPE) and other thermodynamic properties at the MP2/6-31G\* level using Scott and Radom vibrational scaling factors [17]. This completes the determination of the global minimum at the MP2 level. As further

fine tuning we have also performed single-point fourth-order Møller–Plesset perturbation theory including single, double, and quadruple substitution (MP4) and coupled-cluster theory restricted to single, double, and quadruple substitution [CCSD(T)] energy calculations on some of the low-energy MP2 optimized geometries.

All the MP2 and AM1 calculations were performed using the GAMESS program [18]. The MP2 calculations were performed using a 6-31G\* basis set [19, 20]. Honea et al. [21] used the same MP2/6-31G\* method to calculate the Raman frequencies of  $\text{Si}_y$  ( $y = 4, 6, 7$ ), which are consistent with the experimental frequencies. Li et al. [22] also used the same method to compute IR frequencies for the  $\text{Si}_6$  clusters, and their theoretical results agree well with the experimental results [22]. The GAM1 semiempirical calculations were also performed using a slightly modified version of the GAMESS program, which enabled the inclusion of the GAM1 parameters for the Si atom. The MP4 and CCSD(T) calculations were performed using the Gaussian 94 package [23]. The PGA and CGA optimizations were performed with computer codes developed by us.

---

## Results and Discussion

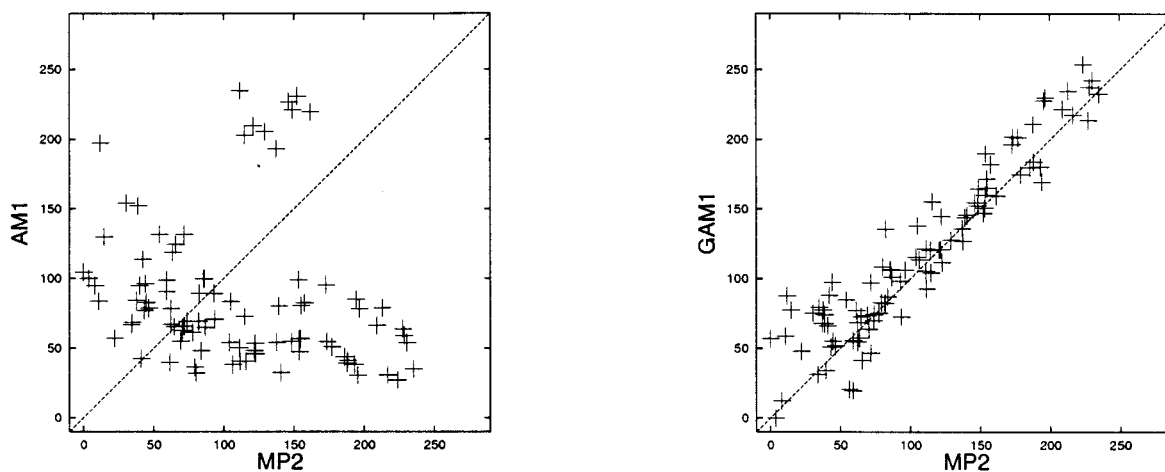
We illustrate our strategy for two different silicon hydride clusters with low and medium H passivation:  $\text{Si}_6\text{H}_2$  and  $\text{Si}_6\text{H}_6$  clusters. The original AM1 and the two sets of final GAM1 Si atom parameters are tabulated in Table I. The GAM1 Si atom parameters optimized for the  $\text{Si}_6\text{H}_6$  cluster stoichiometry are generally closer to the AM1 parameters than are the GAM1 parameters obtained from the  $\text{Si}_6\text{H}_2$  clusters. This is not surprising, because the original AM1 Si parameters were obtained using mostly compounds where the Si atoms were four-coordinate bonded [8]. The Si GAM1 parameters determined for the  $\text{Si}_6\text{H}_2$  clusters show large increases in the core integrals  $U_{ss}$  and  $U_{pp}$  and the resonance parameters  $\beta_s$  and  $\beta_p$  and is probably a reflection of the greater degree of multiple Si–Si bonding taking place in these clusters. For both cluster types we find the core repulsion parameters  $L_1$ ,  $L_2$ , and  $L_3$  to adopt a wide range of values during the GAM1 parametrization runs, to confirm the original expectation that these parameters play a less important role in getting the correct energy in the original AM1 method [5].

**TABLE I**  
**Comparison of the AM1 and the final Si<sub>6</sub>H<sub>2</sub> and Si<sub>6</sub>H<sub>6</sub> GAM1 parameters.**

Parameters	AM1	GAM1(Si <sub>6</sub> H <sub>2</sub> )	GAM1(Si <sub>6</sub> H <sub>6</sub> )
U <sub>ss</sub> /eV	-33.953622	-42.809285	-34.499993
U <sub>pp</sub> /eV	-28.934749	-31.966910	-26.766126
ζ <sub>s</sub> /a.u.	1.830697	1.456994	1.450233
ζ <sub>p</sub> /a.u.	1.284953	1.315649	1.265556
β <sub>s</sub> /eV	-3.784952	-5.248804	-4.359965
β <sub>p</sub> /eV	-1.968123	-4.419519	-2.560926
α/Å <sup>-1</sup>	2.257816	2.352404	2.183698
K <sub>1</sub>	0.250000	0.305731	0.281696
K <sub>2</sub>	0.061513	0.072892	0.098506
K <sub>3</sub>	0.020789	0.026816	0.017541
L <sub>1</sub>	9.000000	10.012125	19.046254
L <sub>2</sub>	5.000000	5.522481	4.288868
L <sub>3</sub>	5.000000	2.014358	7.737797
M <sub>1</sub>	0.911453	1.351186	0.995406
M <sub>2</sub>	1.995569	1.807782	1.510432
M <sub>3</sub>	2.990610	2.875304	1.655458

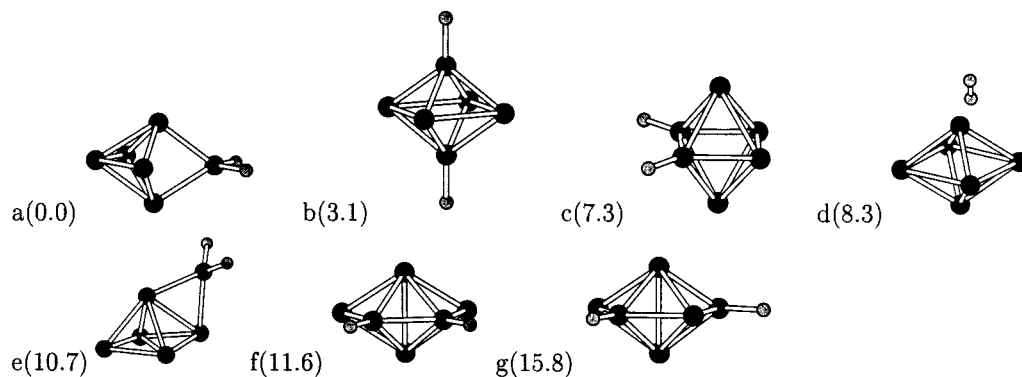
### Si<sub>6</sub>H<sub>2</sub>

Figure 1 compares the AM1 and GAM1 relative energies against the MP2 relative energies for all the Si<sub>6</sub>H<sub>2</sub> clusters included in final training set. The reparametrized GAM1 method does a good job of approximating the energy ranking given by the MP2 relative energies, whereas the AM1 relative energies hardly show any linear relationship when compared against the MP2 relative energies. The AM1 Si<sub>6</sub>H<sub>2</sub> global minimum has a linear structure and is 211 kcal/mol less stable than the lowest MP2 energy cluster we locate at the MP2 level.



**FIGURE 1.** The AM1 and GAM1 versus MP2 relative energies for the Si<sub>6</sub>H<sub>2</sub> clusters. All energies are in kcal/mol.

Figure 2 shows the seven most stable Si<sub>6</sub>H<sub>2</sub> structures, within the 20 kcal/mol range, that we obtained at the MP2 level. It is worth noting that in Figure 2 we draw lines connecting two Si atoms to suggest there is a bond formed when the distance between the two Si atoms is less than 2.8 Å. The relative MP2 energies (including ZPE) of these Si<sub>6</sub>H<sub>2</sub> structures are included in the parentheses after each label, in increasing order. Structure 2(a)—consisting of an elongated Si<sub>6</sub> octahedron, with elongation occurring for the Si atom bound to the two H atoms—is what we determine to be the global minimum at the MP2 level. The C<sub>s</sub> structure in Figure 2(e) was previously determined as the MINDO/3 global minimum by Meleshko et al. [2]. Thus, our method finds four ab initio structures, Figure 2(a–d), that are more stable than the MINDO/3 global minimum, by 10.7, 7.6, 3.4, and 2.4 kcal/mol, respectively. It is worth noting that structure 2(d) has the H<sub>2</sub> molecule separated from the Si<sub>6</sub> framework and corresponds to Si<sub>6</sub>H<sub>2</sub> losing H<sub>2</sub>. Others identified the D<sub>4h</sub> Si<sub>6</sub> compressed octahedron structure 2(d) the Si<sub>6</sub> global minimum and it has been characterized experimentally by Raman and IR spectroscopy [21, 22]. However, our Si<sub>6</sub> in structure 2(d) is slightly distorted from the D<sub>4h</sub> symmetry, owing to the presence of the H<sub>2</sub> molecule about 3.7 Å away from the nearest Si atom. The fact that we find structure 2(d) suggests that even though the GAM1 parameter set is optimized for the Si<sub>6</sub>H<sub>2</sub> stoichiometry, it can still provide a reasonable estimate of the relative stabilities of the clusters with different stoichiometries and slightly lower H passivation. Structures 2(a–c) and 2(f) are



**FIGURE 2.** The  $\text{Si}_6\text{H}_2$  MP2 optimized structures within 20 kcal/mol of the global minimum found by the global optimization procedure. The structures are labeled in order of increasing energy, where the numbers in the parentheses are the MP2 energies with ZPE corrections given in kcal/mol relative to structure (a). Structure (e) is the MINDO/3 global minimum previously found by Meleshko et al. [2].

the four most stable clusters investigated by Chambreau et al. [1] and which were obtained by initially adding H atoms onto the  $D_{4h}$   $\text{Si}_6$  framework. The authors used Gaussian (G3) theory [24, 25] to evaluate the relative energies of the above clusters and ranked the structures 2(a–c) in the reverse energy order to our ranking. Their relative energies (including ZPE) of the structures 2(a–c) are 0.0,  $-1.2$ , and  $-2.2$  kcal/mol, respectively. However, our MP2 calculations still agree with their G3 calculations by ranking the structures 2(a–c) as the most stable structures within 8 kcal/mol of each other. When we further evaluate the MP4 and CCSD(T) single-point energies at the MP2 optimized geometries we obtain 2(a), 2(b), and 2(c) relative energies (including ZPE) of 0.0, 1.9, and 5.7 kcal/mol with MP4 and 0.0,  $-0.8$ , and 2.9 with CCSD(T), showing that there are small energy differences between all

three structures. The calculations by Chambreau et al. suggest that the strategy of fabricating low-energy  $\text{Si}_6\text{H}_2$  clusters from the stable  $\text{Si}_6$  framework is a reasonable one, but in addition to the vertical compression and horizontal expansion of the  $\text{Si}_6$  framework found in 2(f) and 2(g) our global optimization strategy demonstrates the ability to find another low-energy  $\text{Si}_6\text{H}_2$  structure 2(e), which has a very different  $\text{Si}_6$  framework. All seven of the low-energy structures shown in Figure 2 are about 200 kcal/mol at the MP2 level more stable than the global minimum structure found using AM1.

### $\text{Si}_6\text{H}_6$

The two charts in Figure 3 show the deviation of the (G)AM1 relative energies from the MP2 relative energies for all the  $\text{Si}_6\text{H}_6$  clusters in the final train-

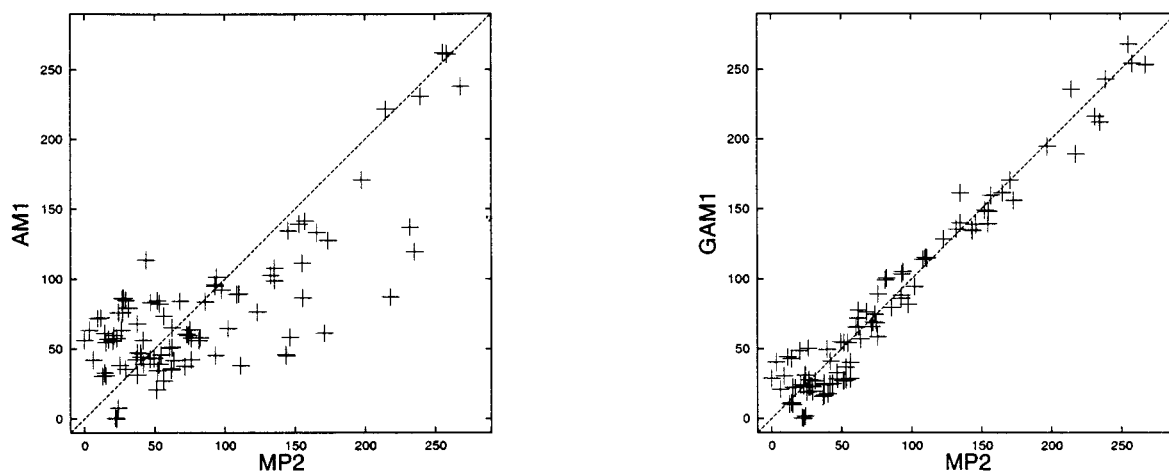


**FIGURE 3.** The AM1 and GAM1 versus MP2 relative energies for the  $\text{Si}_6\text{H}_6$  clusters. All energies are in kcal/mol.

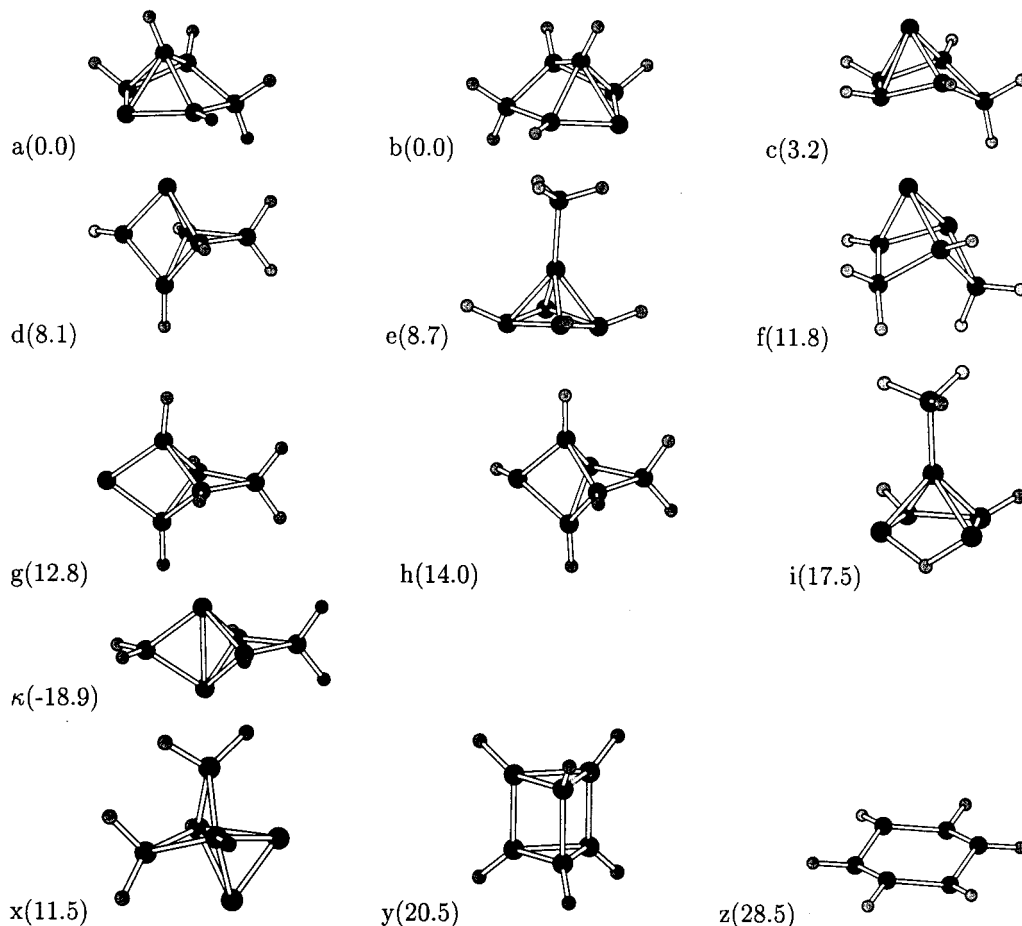


**FIGURE 4.** The  $\text{Si}_6\text{H}_6$  MP2 optimized structures. Structures (a–i) were obtained by our global optimization procedure and are labeled in order of increasing energy, where the numbers in the parentheses are the MP2 energies with ZPE corrections given in kcal/mol relative to structure (a). Structure ( $\kappa$ ) is the lowest-energy structure found by Miyazaki et al. related to structures (d), (g), and (h) by different H atom arrangements. Structures (x–z) are additional low-energy structures previously found by Meleshko et al. and Miyazaki et al. [2, 3].

ing set. The AM1 method does a better job at getting relative energies for the  $\text{Si}_6\text{H}_6$  clusters than it did for the  $\text{Si}_6\text{H}_2$  clusters with lower H passivation. However, the new GAM1 parameters dramatically improve the linear relationship between the semiempirical and the MP2 energies.

Figure 4 shows the nine lowest MP2 energy clusters (a–i) within the 20-kcal/mol range we have located by our global optimization method. We also include in Figure 4 three low-energy  $\text{Si}_6\text{H}_6$  structures (x–z) described previously by Meleshko et al. [2] and the four structures ( $\kappa$ , x–z) discussed by Miyazaki et al. [3]. Overall, we find the Miyazaki et al. ( $\kappa$ ) structure to be the cluster with lowest energy in Figure 4 but, as we discuss below, ( $\kappa$ ) is closely related to structures 4(d), 4(g), and 4(h) found by us. The MP4 and CCSD(T) single-point energy cal-

culations on the MP2 optimized geometries shown in Figure 4 provide the same energy ranking as does the MP2 calculations, apart for structure 4(g), which becomes 1.1 (MP4) and 3.4 [CCSD(T)] kcal/mol more stable than 4(f). As a result of the GAM1 reparametrization, all our identified low-energy structures 4(a–i) are more stable than structure 4(y), which was found to be the AM1 global minimum.

The nine low-energy structures 4(a–i) exhibit three different types of  $\text{Si}_6$  frameworks, where each of these frameworks are surrounded by various arrangements of the 6 H atoms. The Si framework in structures 4(a), 4(b), 4(c), and 4(f) consists of a  $\text{Si}_5$  ring with one Si atom above. Structures 4(d), 4(g), and 4(h) contain a bipyramidal  $\text{Si}_5$  cluster, with the sixth Si atom bridging two of the equatorial Si atoms. The 4( $\kappa$ ) structure also has this  $\text{Si}_6$  framework. Finally, structures 4(e)

and 4(i) are built on a  $\text{Si}_5$  tetragonal pyramid with a silyl,  $\text{SiH}_3$ , group attached to the top the pyramid. Clearly, these Si frameworks in  $\text{Si}_6\text{H}_6$  are very different from those found for low-energy  $\text{Si}_6\text{H}_2$  clusters, and this must be a consequence of the higher opportunity for Si to achieve tetravalency provided by the four extra H atoms. It is interesting that none of the 4(a–i) structures found by our cluster optimization strategy contain any of the  $\text{Si}_6$  frameworks that occur in structures 4(x), 4(y), and 4(z). We find the 4(y)  $\text{Si}_6$  framework type, but because its MP2 relative energy exceeds our 20 kcal/mol energy retention threshold, we do not include it with the other low-energy structures found during the global optimization. The lower ab initio energy of structure 4(x) suggests it might be expected to be among our final set of low-energy structures. Unfortunately, 4(x) is eliminated from ab initio consideration because its optimized GAM1 energy is 36.9 kcal/mol higher than for the 4(a) and 4(b) structures, where even this GAM1 energy represents a big improvement over the 64.7 kcal/mol calculated for the optimized AM1 structure.

The  $\text{Si}_6$  framework plays the primary role in determining the relative energies of the different the  $\text{Si}_6\text{H}_6$  clusters, with the energy of a specific cluster appearing to be finer tuned by the H atom arrangement around the  $\text{Si}_6$  framework. For instance, our global minimization strategy locates the degenerate structures 4(a) and 4(b), which are enantiomers of each other. Structure 4(c) is 3.2 kcal/mol higher in energy as the H atom on the top Si atom shifts to a Si atom in the  $\text{Si}_5$  ring. There is a slightly larger energy change as two  $\text{SiH}_2$  groups are formed in 4(f) while decreasing the number of Si—Si bonds between the top Si atom and the  $\text{Si}_5$  ring atoms. In 4(c) this Si—Si bond length was 2.5 Å and in 4(f) the top Si atom is 3.4 Å from the Si atom in the  $\text{SiH}_2$ . Likewise, for structures 4(e) and 4(i), we find a 8.8 kcal/mol MP2 energy increase as one of the basal H atom shifts from a Si—H bond to bridging a pair of Si atoms. Structure 4(i) is a true local minimum representing an intermediate structure connecting 4(e) to another (e)-like structure but with the H atom shifted to the neighboring unpassivated basal Si atom, suggesting that there are relatively low barriers to H atom rearrangement on the  $\text{Si}_6\text{H}_6$  clusters.

We could present the same kind of discussion for the different H atom arrangements on clusters 4(d), 4(g), 4(h), and 4( $\kappa$ ), except that ( $\kappa$ ) is significantly lower in energy than is our global minima 4(a) and 4(b) as well as (d). One explanation for the lower stability of 4( $\kappa$ ) becomes apparent when one notes that (g) and (h) have two H atoms each bound to both apical Si atoms in the  $\text{Si}_5$  bipyramid, structure 4(d) has

lower energy because there is only one H atom bound to one of the available apical Si atoms. In 4( $\kappa$ ) there are no H atoms binding with either apical Si atoms and the distance between the two apical Si atoms is reduced to 2.71 Å, suggesting that they are starting to form a Si—Si bond. Miyazaki et al. [3] initially chose to investigate the 4( $\kappa$ ) structure because the  $\text{Si}_6$  framework corresponds to the “tetrahedral-bond-network” (TBN) structure designation by Patterson and Messmer [26].

Using our global optimization strategy, it is difficult to find the 4( $\kappa$ ) structure, for two main reasons. The AM1 optimized 4( $\kappa$ ) structure is 12.2, 14.4, and 20.2 kcal/mol less stable than the 4(d), 4(g), and 4(h) structures, and although we improve the energy ranking with our final GAM1 parameters 4( $\kappa$ ) is still 7.8, 19.7, and 7.5 kcal/mol higher in energy than the 4(d), 4(g), and 4(h) structures, respectively. As a consequence, 4( $\kappa$ ) is never selected to join the parametrization training set so that it can more easily be identified as one of the lower energy structures. Second, although the three mating operations we use to make new generations of structures in our CGA appear to be good at finding the different low-energy  $\text{Si}_x$  frameworks, these mating operations do this while retaining many of the Si—H bonds. As a consequence, the current CGA explores many different  $\text{Si}_x$  frameworks but only a subset of the possible H atom arrangements on these frameworks. Our work demonstrates the well-known feature that GAs are good tools for searching for the lower-energy local minimum on a potential energy hypersurface, but the rate of convergence of the genetic algorithm towards the global minimum is not necessarily enhanced by information from any of the low-energy structures closely related to the global minimum [27]. However, a good feature of the current iterative global optimization strategy is that it enables us to identify the energetically important  $\text{Si}_x$  frameworks in the  $\text{Si}_x\text{H}_y$  clusters. We are currently working on developing an improved strategy for examining different H atom arrangements on these Si frameworks. Even with the current procedure, after visually inspecting the different H atom arrangements on a specific  $\text{Si}_x$  framework, it would not be too laborious a task to manually check a few closely related structures for the possibility that they have lower energies.

---

## Conclusion

We have attempted to develop a strategy for the global optimization of binary  $\text{Si}_x\text{H}_y$  clusters at the

ab initio level using two coupled genetic algorithms. One GA (CGA) searches among the many structure candidates for potential low-energy clusters via fast semiempirical calculations so that the energy of only a few structures—including, it is hoped, the global minimum—need to be evaluated using ab initio MP2/6-31G\* calculations. Because semiempirical calculations can often give a different energy ranking to the ab initio ranking, we use a second GA (PGA) to reparametrize the semiempirical method as different new ab initio structures with low energy appear from the CGA.

To illustrate our global optimization strategy, we have attempted to find the ab initio global minima for the  $\text{Si}_6\text{H}_2$  and  $\text{Si}_6\text{H}_6$  clusters. Reparametrizing AM1 for specific  $\text{Si}_x\text{H}_y$  stoichiometries certainly improves the ability of the semiempirical method to rank the energy of different structure types. For  $\text{Si}_6\text{H}_2$  we found seven low MP2 energy structures within 20 kcal/mol of each other. The global minimum has the two H atoms attached to a single Si atom on a distorted  $\text{Si}_6$  octahedron. Our  $\text{Si}_6\text{H}_2$  global minimum is over 10 kcal/mol more stable than the MP2 energy of the global structure previously found by Meleshko et al. [2] using MINDO/3 calculations. Our results for  $\text{Si}_6\text{H}_6$  are more complicated and we find nine lowest MP2 energy structures within 20 kcal/mol of each other. Unfortunately, none of structures correspond to the structure that is 18.9 kcal/mol lower in energy, and presumably the global minimum, found previously by Miyazaki et al. [3]. Nonetheless, our global optimization strategy does find several  $\text{Si}_6\text{H}_6$  clusters with the same  $\text{Si}_6$  framework as the global minimum but with different H atom arrangements. Suggestions for manual checks of possible lower-energy structures can be made by visually inspecting the H atom arrangements on the Si framework.

Our experience with the  $\text{Si}_6\text{H}_2$  and  $\text{Si}_6\text{H}_6$  clusters suggests that we have developed a useful and efficient ab initio global optimization strategy. For the binary  $\text{Si}_x\text{H}_y$  clusters the method is especially useful for finding the important low-energy  $\text{Si}_x$  frameworks and are now trying to develop a better procedure for investigating the best arrangement the H atoms can adopt around the Si framework.

#### ACKNOWLEDGMENTS

The authors are grateful for the generous use of the IBM SP2 at the Maui High Performance Computer Center and the SP2 donated to the University of Hawaii by IBM.

#### References

1. Chambreau, S. D.; Wang, L.; Zhang, J. *J Phys Chem A* 2002, 106, 5081.
2. Meleshko, V.; Morokov, Y.; Schweigert, V. *Chem Phys Lett* 1999, 300, 118.
3. Miyazaki, T.; Uda, T.; Stich, I.; Terakura, K. *Chem Phys Lett* 1996, 261, 346.
4. Ge, Y.; Head, J. D. *J Phys Chem B* 2002, 106, 6997.
5. Dewar, M. J. S.; Zoebisch, E. G.; Healy, E. F.; Stewart, J. J. P. *J Am Chem Soc* 1985, 107, 3902.
6. Møller, C.; Plesset, M. S. *Phys Rev* 1934, 46, 618.
7. Becke, A. D. *J Chem Phys* 1993, 98, 5648.
8. Dewar, M. J. S.; Jie, C. *Organometallics* 1987, 6, 1486.
9. Rossi, I.; Truhlar, D. G. *Chem Phys Lett* 1995, 233, 231.
10. Stewart, J. J. P. *J Comput Chem* 1989, 10, 209.
11. Cundari, T. R.; Deng, J.; Fu, W. *Int J Quantum Chem* 2000, 77, 421.
12. Hartke, B. *Chem Phys Lett* 1996, 258, 144.
13. Stillinger, F. H.; Weber, T. A. *Phys Rev B* 1985, 31, 5262.
14. Gong, X. G. *Phys Rev B* 1993, 47, 2329.
15. Bolding, B. C.; Anderson, H. C. *Phys Rev B* 1990, 41, 10568.
16. Hartke, B. *Theoret Chem Acc* 1998, 99, 241.
17. Scott, A. P.; Radom, L. *J Phys Chem* 1996, 100, 16502.
18. GAMESS, The General Atomic and Molecular Electronic Structure System; Schmidt, M. W.; Baldridge, K. K.; Boatz, J. A.; Elbert, S. T.; Gordon, M. S.; Jensen, J. H.; Koseki, S.; Matsunaga, N.; Nguyen, K. A.; Su, S.; Windus, T. L.; Dupuis, M.; Montgomery, J. A., Jr. *J Comput Chem* 1993, 14, 1347.
19. Francl, M. M.; Pietro, W. J.; Hehre, W. J.; Binkley, J. S.; Gordon, M. S.; Defrees, D. J.; Pople, J. A. *J Chem Phys* 1982, 77, 3654.
20. Hehre, W. J.; Ditchfield, R.; Pople, J. A. *J Chem Phys* 1972, 56, 2257.
21. Honea, E. C.; Ogura, A.; Murray, C. A.; Raghavachari, K.; Sprenger, W. O.; Jarrold, M. F.; Brown, W. L. *Nature* 1993, 366, 42.
22. Li, S.; Van Zee, R. J.; Weltner, W., Jr.; Raghavachari, K. *Chem Phys Lett* 1995, 243, 275.
23. Frisch, M. J.; Trucks, G. W.; Schlegel, H. B.; Gill, P. M. W.; Johnson, B. G.; Robb, M. A.; Cheeseman, J. R.; Keith, T. A.; Petersson, G. A.; Montgomery, J. A.; Raghavachari, K.; Al-Laham, M. A.; Zakrzewski, V. G.; Ortiz, J. V.; Foresman, J. B.; Cioslowski, J.; Stefanov, B. B.; Nanayakkara, A.; Challacombe, M.; Peng, C. Y.; Ayala, P. Y.; Chen, W.; Wong, M. W.; Andres, J. L.; Replogle, E. S.; Gomperts, R.; Martin, R. L.; Fox, D. J.; Binkley, J. S.; Defrees, D. J.; Baker, J.; Stewart, J. P.; Head-Gordon, M.; Gonzalez, C.; Pople, J. A. *Gaussian 94, Revision E.2*; Gaussian: Pittsburgh, 1995.
24. Curtiss, L. A.; Raghavachari, K.; Redfern, P. C.; Rassolov, V.; Pople, J. A. *J Chem Phys* 1998, 109, 7764.
25. Baboul, A. G.; Curtiss, L. A.; Redfern, P. C.; Raghavachari, K. *J Chem Phys* 1999, 110, 7650.
26. Patterson, C. H.; Messmer, R. P. *Phys Rev B* 1990, 42, 7530.
27. Judson, R. In Lipkowitz, K. B.; Boyd, D. B., Eds. *Reviews in Computational Chemistry*, Vol. 10; VCH: New York, 1999, p. 1.